

DESIGN OF A HIGH-RESOLUTION OPTICAL TRANSITION RADIATION IMAGER FOR THE LINAC COHERENT LIGHT SOURCE UNDULATOR*

B.X. Yang[†], J. L. Bailey, D. R. Walters, and S. J. Stein, ANL, Argonne, IL 60439, U.S.A.

Abstract

The Linac Coherent Light Source (LCLS), a free-electron x-ray laser, is under design and construction. Its high-intensity electron beam, 3400 A in peak current and 46 TW in peak power, is concentrated in a small area (37 micrometer in rms radius) inside its undulator. Ten optical transition radiation (OTR) imagers are planned between the undulator segments for characterizing the transverse profiles of the electron beam. In this paper, we present the performance requirements and technical specifications of the OTR imagers. We will discuss in detail the arrangement and modeling of the imaging optics, and the mechanical design and analysis of the compact camera module. Through a unique optical arrangement, this imager will achieve a fine resolution (12 micrometer rms or better) over the entire field of view (10 mm × 5 mm). The compact camera module will fit in the limited space available with remote focus adjustment. A digital camera will be used to read out the beam images in a programmable region (5 mm × 0.5 mm) at the full beam repetition rate (120 Hz), or over the entire field at a lower rate (15 Hz).

INTRODUCTION

The Linac Coherent Light Source (LCLS), a free-electron x-ray laser, is under design and construction. Ten optical transition radiation (OTR) imagers are planned between the undulator segments for the characterization of the electron beam's transverse profiles [1].

It has been shown that resolutions under 5 μm can be achieved with OTR screens and appropriate optics [2-4]. The technical challenge here is to perform these measurements with the same high resolution, reliability, reproducibility, and accuracy. In this work, we describe a compact, modular imaging system designed to meet this challenge.

DESIGN SPECIFICATIONS

The requirements of the OTR imager is derived from the electron beam parameters in the undulator for the current design, shown in Table 1 [5].

We notice that uncertainties in beam size measurements come from many sources: screen defect, optics defect, optics resolution, calibration error, and photon statistics [6]. Since these uncertainties (resolution) are added to the measured beam radius in quadrature, $\sigma_{EXP} = \sqrt{\sigma_{RES}^2 + \sigma^2}$, the resolution-induced error in measured radius, if uncorrected, would be

$$\left(\frac{\Delta\sigma}{\sigma}\right) \approx \frac{1}{2} \left(\frac{\sigma_{res}}{\sigma}\right)^2. \quad (1)$$

In this work we take the maximum acceptable error in beam radius as $[\Delta\sigma/\sigma] \sim 5\%$, or 2 – 3 μm, the maximum acceptable resolution is thus 32%, or 12 – 17 μm.

Many of these uncertainties could be corrected by subtracting the resolution (more precisely, the rms width of the point spread function for the entire optical system) from the measured beam size. The true experimental error after the correction is normally a fraction of the “resolution,” usually originating from properties that vary across the field of view or change over time. In this work, we will make a conservative estimate that only 50% of the resolution effect is correctable, and the attainable accuracy of the measurement would be better than 2 μm for a total resolution of 12 μm.

Table 1: Beam Parameters in the LCLS Undulator [5]

Electron energy (GeV)	4.313	13.640
Single bunch charge (nC)	0.2 – 1.0	0.2 – 1.0
Normalized emittance (μm-rad)	3.0	2.0
Average beta function (m)	10.3	28.7
Rms beam size (μm)	55	37
Chamber size (mm)	10 mm (H) × 5 mm (V)	

OPTICS DESIGN

Geometry

Most OTR screens in use employ a large incidence angle (~ 45°) for the electron beam. Every time the beam moves away from the screen center, the imager is out of focus. Murokh et al. [7] used an annular parabolic mirror in a normal-incidence geometry to solve the problem (Fig. 1A). It can be slightly altered to use a plane mirror-achromat combination (Fig. 1B) to reduce the cost and improve flexibility of optics design, at the expense of increased chromatic aberration. But the hole in the mirror makes them unsuitable for a high-energy electron beam, since a good fraction of OTR light would be lost through the hole.

We then considered two other alternatives of using near-normal incidence OTR screen (Fig. 1C and D). To compensate the slight tilt angle ($\psi \sim 5^\circ$) of the object plane, we also need to tilt the camera (ψ'). The two angles are related by $\tan\psi' = M \tan\psi$, since the longitudinal magnification is M^2 for a lens system with a transverse magnification of M . Tilting of the image plate was a standard feature in many large cameras beginning in the late 19th century, and it has been in use for beam

*Work supported by the U.S. Dept. of Energy, under contract numbers W-31-109-ENG-38 and DE-AC03-76SF00515.

[†]bxyang@aps.anl.gov

diagnostics for at least ten years [8]. It is only practical in this case because the tilt angle of the screen is small. We decided to start with the plane mirror and lens as our base design due to its simplicity.

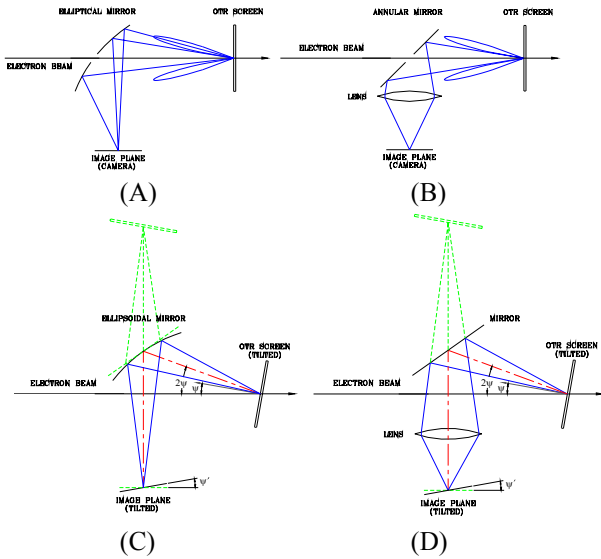


Figure 1: OTR imager optics arrangements to maintain focus in full screen: (A) off-axis ellipsoid mirror; (B) plane mirror-achromatic lens combination; (C) off-axis ellipsoid mirror with tilted screen and camera; and (D) similar to C but using plane mirror and lens.

Efficiency

From the angular distribution of the OTR light

$$E(\theta) \approx \frac{\mu_0 e c \beta}{\sqrt{2\pi R}} \cdot \frac{\tan \theta}{\cos \theta (\tan^2 \theta + \gamma^{-2})}, \quad (2)$$

one can derive the photon flux through an angular cone of radius θ_0 . For ultra-relativistic particles ($\gamma \gg 1$), the absolute efficiency $\eta(\theta_0)$, defined as the ratio of this flux to all that is available ($\theta < \pi/2$), can be written as

$$\eta(\theta_0) \approx \frac{1}{\ln 4\gamma^2 - 1} \left[\ln \left(1 + 4\gamma^2 \tan^2 \frac{\theta_0}{2} \right) + \frac{\cos \theta_0}{1 + \gamma^2 \sin^2 \theta_0} - 1 \right]. \quad (3)$$

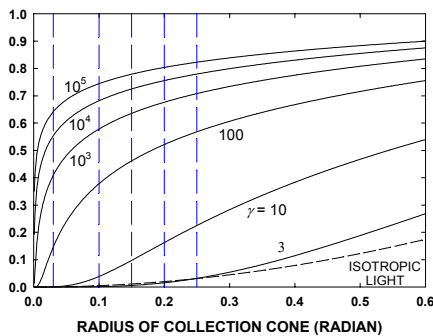


Figure 2: Light efficiency of OTR imager for selected electron energy ($E = \gamma m_e c^2$).

Figure 2 shows the efficiency as a function of collection angle. Note that the electron energy of LCLS is in the

range of $\gamma \sim 10^4$, so we selected a collection cone radius of 0.075-radian ($\gamma\theta_0 = 750$) as our base design. Any increase will have only minimal gain in light efficiency.

Diffraction-Limited Resolution

Applying Huygens principle on the angular distribution of the OTR light, Eq. (1), an approximate point spread function (PSF) can be derived [2],

$$|E_x|^2 \propto \left(\frac{1 - J_0(x/\Lambda_0)}{x/\Lambda_0} \right)^2, \quad (\Lambda_0 = \lambda/\theta_0). \quad (4)$$

The PSF is a ring with a radius $\sim 2.8 \cdot \Lambda_0$ (Figure 3A). Integration of the intensity over y -coordinates resulted in a double-peaked profile of x -coordinates (Figure 3B). Fitting the profile to Gaussian functions [9] results in a Gaussian radius of $4.2 \cdot \Lambda_0$, which is ~ 3.5 times the Gaussian radius of the PSF if the same optics are used to image an isotropic point source ($\sim 1.2 \cdot \Lambda_0$). Inserting a y -polarizer could further improve the resolution in the x -direction by about a factor of two [3,4].

For a 0.075-radian collection cone radius, the length unit Λ_0 is within 0.8 – 1.4 μm in the visible light region. Hence the diffraction-limited Gaussian radius is in the range of 3.5 – 6 μm .

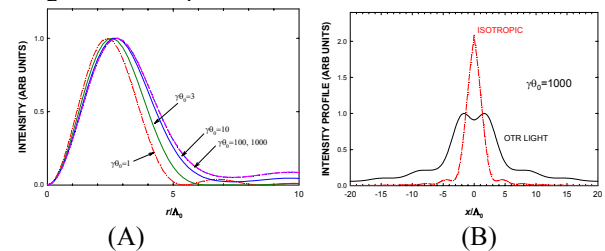


Figure 3: Diffraction-limited OTR intensity distributions: (A) point spread function in radial coordinates, (B) vertically integrated profile.

Aberration Estimate

Optical aberrations were estimated using a ray-tracing program ZEMAX. Achromatic doublets (300-mm focal length) from several manufacturers were tested. For some wavelength ranges, a mixture from different vendors yields slightly better results. Table 2 summarizes the geometric ray-tracing results.

Table 2: Ray-Tracing Results Summary (48-mm aperture)

Wavelength range	RMS spot radius
550 nm (monochromatic)	1.6 μm
565 – 635 nm	6 μm
500 – 700 nm	10.5 μm
400 – 700 nm	22 μm

It can be seen that the chromatic aberration has the dominant contribution, and a bandpass filter is desired if we want to match the geometric aberration to the diffraction limit. However, since the OTR has anisotropic distribution, we expect the actual aberration will be better

than Table 2 indicates. In places where best resolution and best efficiency are needed at the same time, we will implement the focusing mirror approach in Figure 1C.

MECHANICAL DESIGN

We took a modular approach in the opto-mechanical design of the OTR imager. Figure 4 shows the OTR imager's test assembly. A custom vacuum cube is used to maintain the vacuum integrity for the beamline and provide precisely machined mounting surfaces. The OTR screen is supported by a feedthrough, which is mounted at 5-degree angle from the vertical line. The OTR light is collected by an in-vacuum mirror and steered into the camera module. A pair of 50-mm achromatic lenses produces an image at the CCD camera at a magnification of 1. The first lens is mounted on a fixed enclosure, which can be adjusted in the transverse direction to center the image. The second lens is mounted on a longitudinal translation stage driven by a stepper motor to provide remotely controlled focus. The CCD camera is tilted at 5 degrees to compensate for the tilt of the OTR screen. The enclosures of the CCD camera and the last two lenses are made of tungsten alloy to provide radiation shielding for the CCD sensor. The CCD camera was selected from Imperx CCD lines for their following features:

- At 7.4 μm per pixel, the 1024 \times 2048 elements of the cameras enable us to obtain the required resolution while covering the entire field of view (10 \times 5 mm²)
- The cameras are equipped with programmable electronic gains from 0.03 to 36. This will enable the camera to operate over 0.1 – 1.0 nC change range without a need for a remotely adjustable iris aperture or an ND filter set.
- While their full-screen frame rate is 15 Hz, their region-of-interest readout feature will allow imaging at full beam pulse rate (120 Hz) at a reduced field of view.

SUMMARY

We have completed the optical and mechanical design of the OTR imager used in the LCLS undulator. Through a unique optical arrangement, this imager will achieve 12- μm resolution over the entire field of view (10 mm \times 5 mm) and for bunch charge ranging from 0.1 nC to 1.0 nC.

REFERENCES

- [1] J. Arthur et al., "LCLS Conceptual Design Report," SLAC-R-593, <http://www-ssrl.slac.stanford.edu>.
- [2] V.A. Lebedev, Nucl. Instrum. Methods A372 (1996) 344.
- [3] M. Castellano, and V. A. Verzilov, Phys. Rev. ST Accel. Beams 1, 062801 (1998).
- [4] M. Ross et al., "Very High Resolution Optical Transition Radiation Beam Profile Monitor," BIW02, BNL, May 2002, AIP Conf. Proc. 648, p. 237.

- [5] H. Nuhn, "LCLS Undulator Requirements," LCLS Specification 1.4-001.
- [6] B. X. Yang et al., "Design and Performance of a Compact Imaging System for the APS Linac Bunch Compressor," PAC'01, Chicago, June 2001, p. 2335.
- [7] A. Murokh et al., "Limitations on Measuring a Transverse Profile of Ultra-Dense Electron Beams with Scintillators," PAC'01, Chicago, June 2001, p. 1333.
- [8] A. Specka et al., "High Resolution Beam Monitoring with Optical Transition Radiation at 3 MeV Electron Energy," PAC'01, Chicago, June 2001, p. 1333.
- [9] B. X. Yang, "Optical System Design for High-energy Particle Beam Diagnostics," BIW'02, BNL, May 2002, AIP Conf. Proc. 648, p. 59.

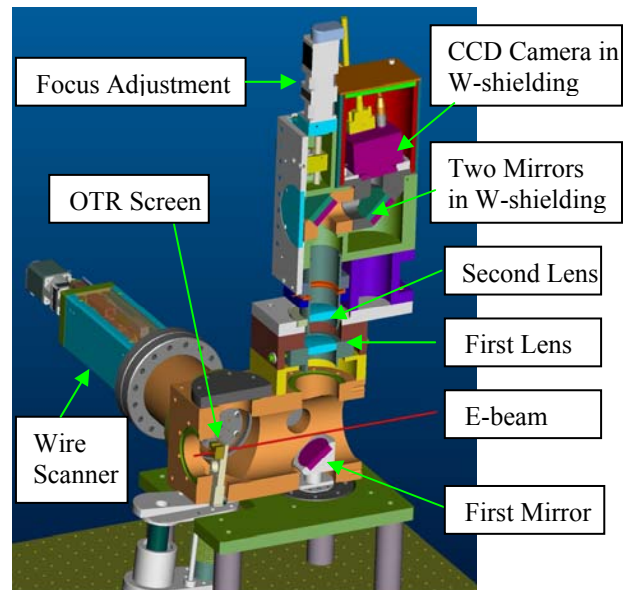


Figure 4: OTR imager and wire scanner test setup.